Quantitative Determination of Glucose Transfer Between Cocurrent Laminar Water Streams in a H-Shaped Microchannel

Michiel van Leeuwen and Xiaonan Li
Dept. of Biotechnology, Delft University of Technology, Kluyver Centre for Genomics of Industrial Fermentation, Delft, The Netherlands

Erik E. Krommenhoek and Han Gardeniers
MESA+ Institute for Nanotechnology, University of Twente, Enschede, The Netherlands

Marcel Ottens, Luuk A. M. van der Wielen, Joseph J. Heijnen, and Walter M. van Gulik
Dept. of Biotechnology, Delft University of Technology, Kluyver Centre for Genomics of Industrial Fermentation, Delft, The Netherlands

To explore the applicability of a laminar fluid diffusion interface (LFDI) for the controlled feeding of microbioreactors, glucose diffusion experiments were carried out in a rounded H-shaped microstructure etched in a glass substrate. The diffusion channel of the microstructure had a length of 4 mm and a depth of 50 µm with a trapezoidal cross section with a width of 100 µm at the bottom and 200 µm at the surface of the channel. The microchannel was operated at residence times of less than 1 s ensuring high-mass-transfer rates. It was confirmed, both by microscopic observations as well as computational fluid dynamics (CFD) studies that the flow characteristics in the microchannel were fully laminar. Special attention was paid to flow splitting at the end of the channel, because the CFD simulations indicated that the performance of the device was sensitive to unequal flow splitting. The difference in outflow volume of the two streams was measured to be small (1.25% ± 0.6%). The measured glucose concentration in both exit ports at a fixed residence time was found to be stable in time and reproducible in multiple experiments. CFD simulation was shown to be a powerful tool for estimating the mass transfer in the LFDI, even at very short residence times. The results obtained in this work show the applicability of LFDI for the controlled diffusive supply of a solute to a water stream, with as possible application substrate and/or precursor feeding to microreactors.© 2009 American Institute of Chemical Engineers Biotechnol. Prog., 25: 1826–1832, 2009
Keywords: microstructure, laminar flow, diffusion interface, mass transfer, glucose

Introduction

Microfluidic devices are becoming powerful tools in analytical and (bio)chemical research because they exhibit unique features and hold the promise to perform high-throughput experiments in extremely small liquid volumes at reduced labor costs.
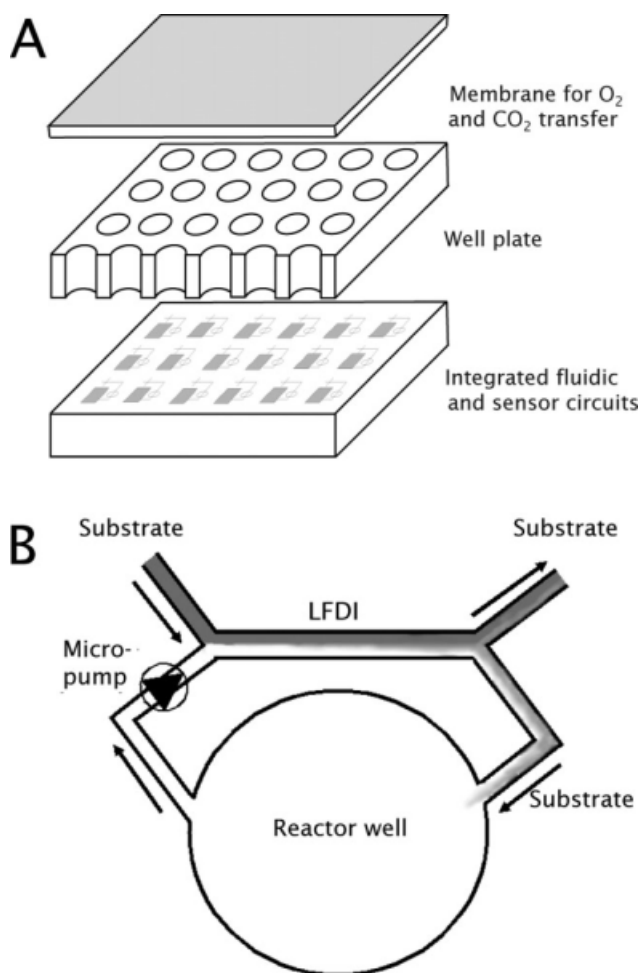
Probably, the most important characteristic of fluids moving through a micrometer-scale channel is the absence of turbulence in the fluid. The Reynolds numbers for liquid flows in microchannels are typically less than 100, indicating a strictly laminar flow regime, whereby diffusion is the predominant transport mechanism. When two miscible streams are introduced in a microchannel, they do not mix but flow in parallel streams, forming a stable liquid–liquid interface over which components can be transferred solely by diffusion. This characteristic feature explains the use of the term laminar fluid diffusion interface (LFDI) for these devices.[1–3] This unique feature of microfluidics is applied for example in enzymatic[4] and chemical conversions[5] that occur at the interface of the two liquid streams, for the measurement of diffusion coefficients[6] and most frequently in separation and extraction processes.[7–10]

So far, the main focus for applicability of LFDI has been on extraction processes, i.e., the H-filter,[8] while the fast and controlled diffusive supply of molecules to a liquid is also very relevant but has been investigated much less. For extraction processes, the design of the LFDI is based on the maximization of the total mass transfer of a desired compound to the receiving stream, while minimizing the transfer of undesired components. For this purpose, relatively long contact times are required. For the fast supply of solutes to a receiving stream, the LFDI should be designed for high-mass transfer rates, requiring a large driving force and thus short contact times.

An interesting application of LFDI could be the diffusive supply of substrates or precursors to microbioreactors, thereby avoiding increase of the reactor volume. Figure 1
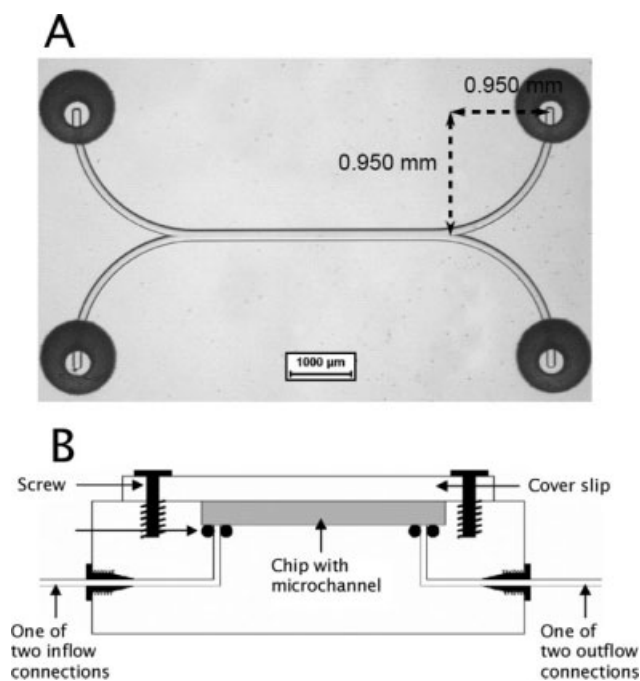
Figure 1. Schematic representation of (A) an array of micro-bioreactors and (B) the application of an LFDI for substrate supply to the reactor wells.

Figure 2. (A) Micrograph of the LFDI chip (top view) and (B) schematic cross section of the chip holder.
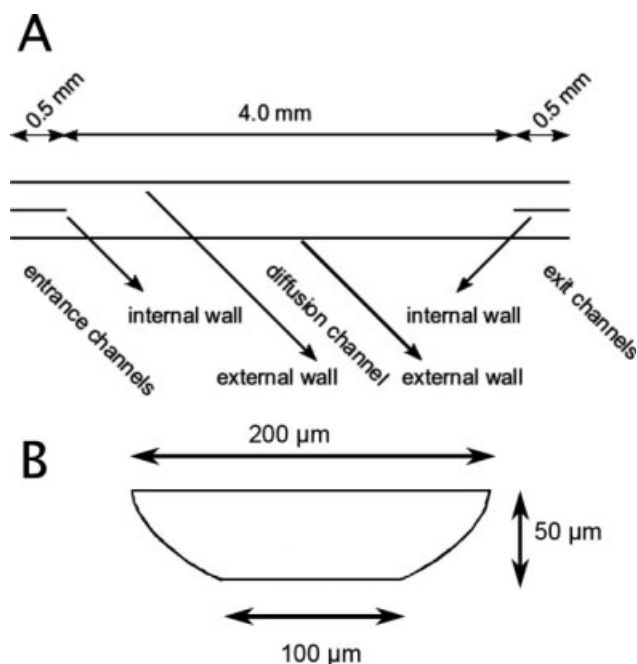
tion at each of the two outflows for multiple hours after the start of the experiments.

Materials and Methods

Design and fabrication of the LFDI

Borofloat (Schott borofloat 33) glass chips with a size of 8×12 mm were obtained from Micronit Microfluics B.V. (Enschede, The Netherlands). In each chip, two channels were etched with a depth of 50 μm joining together to form a single diffusion channel with a length of 4 mm with a subsequent split into two separate channels. To avoid mixing at the point where the two channels joined and to ensure appropriate flow splitting at the end of the diffusion channel, the inlet and outlet channels were designed as quarters of a circle with a radius of 950 μm. Because of the isotropic etching process, the cross section of the channels had a trapezoidal shape. The width of the inlet and outlet channels was 50 μm at the bottom and 150 μm at the top. For the diffusion channel, the widths were 100 and 200 μm at the bottom and the top, respectively. The channels were etched in the Borofloat substrate with 25 wt % hydro fluoric acid solution in water (HF) using a chromium/gold mask as described in Hermes et al.[13] After resist lift-off and thorough cleaning of the glass wafer, it was aligned and bonded to a second glass wafer, using a thermal process. This second glass wafer contained vertical connection channels micromachined by powder blasting. Finally, the bonded pair of glass wafers was diced into individual chips. A picture of an individual chip is shown in Figure 2A.

A chip holder enabling to make the fluidic connections with the chip was fabricated in house (Figure 2B). The chip holder consisted of a PMMA block (width: 37 mm, length: 18 mm, thickness: 10 mm) with a cut away of the size of the chip. The chip was inserted in the cut away and covered with a 1 mm thick PMMA cover slip which was held in position by four screws. Four channels (1 mm diameter) in total were drilled from the left or right side of the chip holder to the powder blasted entrance and exit points on the chip. At the end of the

---

shows a schematic representation of the possible application of an LFDI in a microbioreactor setup.

For the practical application of LFDI devices, three aspects are crucial: (a) a stable liquid–liquid interface, (b) reproducible mass transfer rates, and (c) equal splitting of the two flows at the end of the device. In the current literature on this subject, the focus has been, too a large extent, on the stability of the interface, while little attention has been paid to the quantification of the mass transfer of the device, especially in combination with flow splitting. In most papers addressing the mass transfer of LFDI devices, only the theoretical aspects have been discussed,[1,11] or the solute concentration is directly measured in the channel.[12] Until now, little attention has been paid to the splitting of the streams at the end of the diffusion channel. Unequal flow splitting should be prevented because it will, in the case of a recycle stream from/to a microbioreactor, result in either draining or flooding of the reactor.

In this work, we designed and fabricated an LFDI, based on a rounded H-shaped microchannel, for optimal mass transfer between two water streams. Proper flow splitting was investigated visually by introducing a rhodamine B solution in one of the channels. Using glucose as a model substrate, mass transfer rates were determined for a range of different residence times. The experimentally determined glucose mass transfer rates were compared with computational fluid dynamics (CFD) calculations. The robustness of the setup was checked by measuring the glucose concentra-

Figure 3. **Schematic representation, including dimensions, of the diffusion channel of the LFDI as was used for the CFD simulations.**

(A) top view and (B) cross section.

Figure 4. **Relationship between the volumetric flow rate (per stream), linear flow rate, and residence time.**

four channels, 6-32 coned ports were micromachined in the PMMA to be able to connect steel capillaries (outer diameter: 1/32 inner diameter: 600 μm) using standard headless 6-32 coned fittings (Upchurch Scientific, Oak Harbor, WA). The two steel capillaries that were connected to the entrance channels of the chip were connected to two 2.5 mL glass syringes (SGE Analytical Science Pty., Victoria, Australia) which were placed in a syringe pump (KD Scientific 210, Antec Leyden B.V., Zoeterwoude, The Netherlands). The liquid was collected at the other two capillaries.
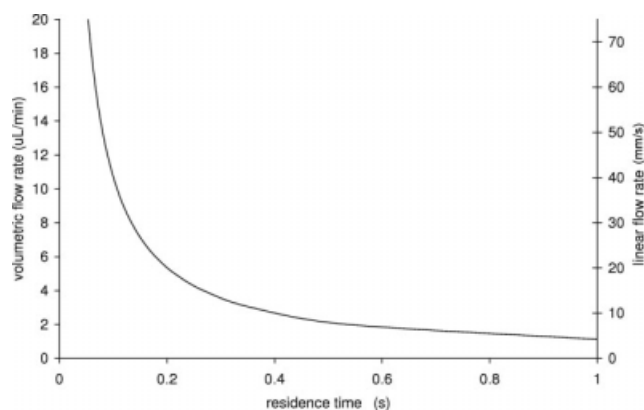
CFD simulations

The three-dimensional (3D) flow and glucose concentration profiles in the microchannel were simulated using the COMSOL 3.3 software package (COMSOL, Sweden). Steady state situations were simulated. The velocity field in the microchannel was first simulated using the Navier-Stokes equations for incompressible fluids (Eqs. 1 and 2). The obtained results were stored and subsequently used in the convection and diffusion equation (Eq. 3), for simulating the glucose mass transfer in the microchannel. The model equations are presented below:

$$\rho \frac{\partial U}{\partial t} - \nabla \cdot \left[\eta \cdot \left(\nabla U + (\nabla U)^T \right) \right] + \rho U \cdot \nabla U + \nabla P = F$$

(1)

$$\nabla \cdot U = 0 \tag{2}$$

$$\frac{\partial c_i}{\partial t} + \nabla \cdot (-D_i \nabla c_i + c_i U) = R_i \tag{3}$$

In the above equations, η denotes the dynamic viscosity of the solution (kg m^{-1} s^{-1}), U denotes the velocity vector (ms^{-1}), ρ denotes the density (kg m^{-3}), P is the pressure (Pa),

c_i denotes the concentration of chemical i in solution (kg m^{-3}), D_i denotes its diffusion coefficient (m^2 s^{-1}), t is time (s) and R_i denotes the reaction term (kg s^{-1} m^{-3}), which equals zero. F denotes the selected volume force field (i.e., gravity). The expression within the brackets in Eq. 3 represents the flux vector, where the first term describes the transport by diffusion and the second represents the convective flux.

To reduce the complexity of the calculation and still gain detailed information on mass transfer and flow profiles from the CFD simulations, only the diffusion channel, in which the actual mass transfer takes place, was simulated over its full 4 mm length. The joining of the two streams and the flow splitting was approached in the simulation by extending the diffusion channel with two sections of 0.5 mm each at the entrance and the exit of the diffusion channel, respectively. In the middle of each of these sections and parallel to the liquid flow, an internal wall (i.e., no slip boundary) was placed to indicate two independent channels (Figure 3). The section at the entrance of the diffusion channel was found to be particularly important to create the appropriate velocity profile at the entrance of the diffusion channel.

The simulation contained 13,988 grid points in total. At the positions of these grid points in the microchannels, the parameters in the Navier Stokes equations plus the solute concentrations were computed at each time step. A finer mesh was used around the point where the two streams combined and split as well as at the contacting plane between both streams over which the mass transfer took place.

For all CFD calculations, pure water was the receiving liquid and an aqueous glucose solution (10.4 mM) was the supply liquid ($D_i = 6.7 \times 10^{-10}$ m^2/s, $\eta = 10^{-3}$ kg m^{-1} s^{-1}, and $\rho = 998$ kg m^{-3}).

Simulations were performed for residence times upto 1 s corresponding to linear flow rates down to 4 mm/s (Figure 4). At steady state conditions, the glucose concentrations in both streams at the end of the diffusion channel were calculated by integration of the two separate 3D glucose concentration profiles at the point of flow splitting. The effect of unequal flow splitting on the glucose concentrations in both exit streams was studied by varying the ratio of the linear flow rates at the exit positions.

Visual verification of the laminar flow regime

The chip holder that was connected to the syringe pump was placed under a microscope and pictures were taken of
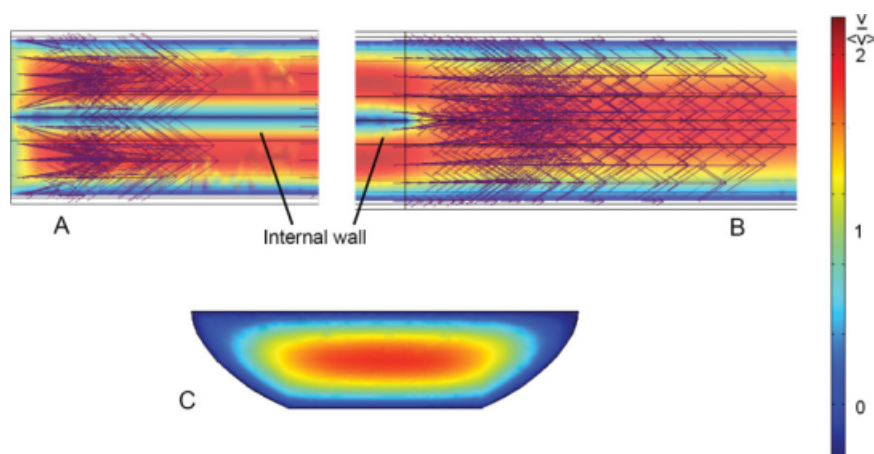
Figure 5. CFD simulation results of the linear flow velocity fields in the diffusion channel at different positions (A) the velocity fields in the two inlet channels, (B) in the diffusion channel at the position where the two channels join, and (C) flow velocity field (cross sectional area) at 1 mm after the two channels join.

The flow rate is indicated by color and is expressed relative to the average velocity as $\frac{V}{<V>}$, with average velocity $<V> = 22.2$ mm/s.
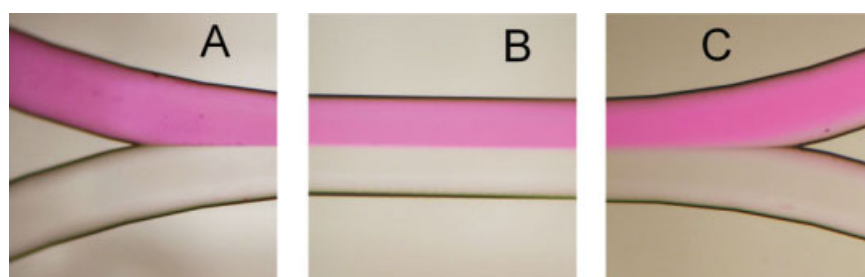
Figure 6. Micrograph of two aqueous streams at the joining point of the streams, halfway the channel, and at the separation point (from left to right); the upper stream is colored with rhodamine B.

The total residence time of the fluid in the diffusion channel was 54 ms.

two concurrent water flows (residence time of 4 ms) in the microchannel of which one of the flows was colored with rhodamine B (2.8 mM).

Mass transfer experiments

For all mass transfer experiments, the supply liquid was an aqueous glucose solution (10.4 mM) and the receiving liquid was demineralized water. Mass transfer experiments were carried out at five different volumetric flow rates, namely 20, 10, 5, 2.5, and 1.25 μL/min per inflow stream, corresponding with residence times in the diffusion channel of 54, 107, 214, 428, and 857 ms. During each experiment, half a dozen samples (75–150 μL) were taken in time from both outlet streams. The glucose concentration in the samples was determined enzymatically (Boehringer Mannheim/ R-Biopharm A.G., Darmstadt, Germany). The enzymatic kit was scaled down for use with 96-well microtiter plates. Absorption was read on a Tecan plate reader (Tecan, Salzburg, Austria). All solutions were prepared freshly and were filtered (Millex®HV, 0.45 μm pore size, Millipore, Ireland) before use.

Results and discussion

The specific interfacial area for mass transfer in the diffusion channel of our LFDI was calculated to be 11.2×10^3 m²/m³. This is three orders of magnitude higher than the specific interfacial area in conventional high-efficiency equipment for liquid/liquid extraction which is in the order of 1–20 m²/m³.[14,15] This clearly shows the advantage of LFDI devices for processes in which high mass-transfer rates are important.

To investigate and predict the mass transfer characteristics of the device, the mass transfer of glucose between two cocurrently flowing water streams was used as a model system. For the practical applicability of such devices, two aspects are crucial: (i) a laminar flow regime, ensuring a stable liquid–liquid interface and well defined mass transfer; and (ii) proper separation of the two liquid streams at the end of the diffusion channel. These aspects are discussed subsequently below.

The flow field

The Reynolds numbers that were calculated for the range of liquid flow rates that were applied in the experiments varied between 1 and 15. These low Reynolds numbers clearly indicate that the flow regime in the microchannel was laminar.

CFD simulations provided detailed information on the flow and velocity patterns in the microchannel (Figure 5). The two entrance channels with a length of 0.5 mm were necessary for developing the parabolic, Hagen-Poiseuille flow profiles before reaching the diffusive channel. The CFD simulations clearly show that the flows were fully developed, well before the point where the two separate channels join (Figure 5A).
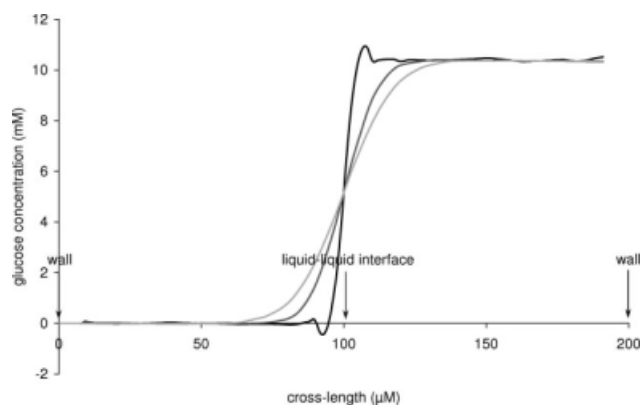
Figure 7. Concentration profiles perpendicular to the flow direction at residence times of 0 (black line), 0.36 (dark gray line), and 0.72 s (light gray line).

Figure 8. CFD simulation of the glucose concentration profile in the diffusion channel, at a cross section located 2 mm after the position were the two inlet channels join, for a residence time of 0.72 s.

The glucose concentration (mM) is indicated by color.

Table 1. The Effect of Unequal Flow Splitting on the Increase in Glucose Concentration in the Receiving Stream, Assuming a Ratio Between the Outflow Rate of the Feed Stream and the Outflow Rate of the Receiving Stream of 0.9

Average Residence Time (ms)	Increase in Glucose Concentration in Receiving Stream (%)
45	47.5
180	19.8
720	8.6

These simulations also indicated that at the joining point, the mass transfer as a result of convective mixing was small, but significant, for residence times below ∼0.5 s (results not shown) and was therefore taken into account in the calculations of the mass transfer rate. However, 0.1 mm downstream of the joining point fully developed parabolic flow was achieved with a stable interface between both water streams (Figure 5B). Because of the dimensions and shape of the channel, the flow was parabolic both across the channel height and width as can clearly be seen in a cross section of the channel (Figure 5C).
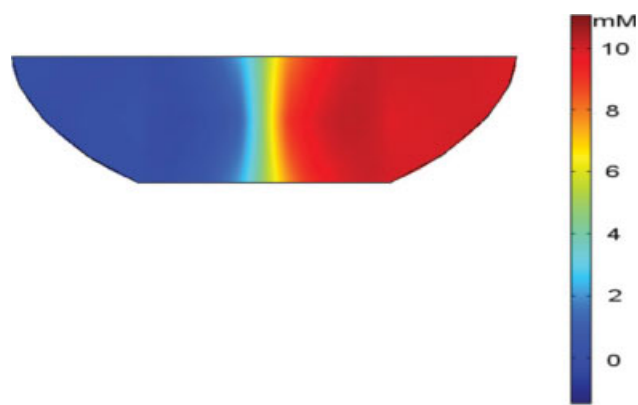
The stable liquid–liquid interface predicted by the CFD simulations was confirmed by the experimental observations. The interface between the two water streams (average residence time of 54 ms) was visualized by coloring one of the streams with rhodamine B and taking micrographs at different positions of the diffusion channel (Figure 6). At the position where the two streams combined, a stable liquid–liquid interface was formed and no turbulent mixing was observed between the two colliding streams. As can be seen from Figure 6, the liquid–liquid interface remained sharp along the entire length of the channel, indicating laminar flow.

The concentration profiles

Because of the difference in glucose concentration between both streams, mass transfer takes place over the contact plane. Provided laminar flow and short residence times, the concentration profile around the contact plane is steep, resulting in a high-mass-transfer rate of glucose between both streams. Short residence times are defined as average residence times in the diffusion channel of less than 1 s.

The glucose concentration profile around the contact plane was calculated from CFD simulations. Figure 7 depicts the simulation results for the glucose profile perpendicular to the channel at different residence times. The simulation results confirm the expected steep concentration profile around the liquid–liquid interface at the joining point. As expected, at larger residence times the concentration profile becomes flatter while the interdiffusive zone broadens. These simulation results were used for the CFD-based estimation of the glucose transfer at different residence times.

The parabolic flow velocity profile in the microchannel induces widening of the interdiffusive zone at the sides where the contact plane between both streams comes near the wall of the channel. This curving of the diffusion front near the wall is sometimes called the butterfly effect.[1] This effect has been shown theoretically from 2D numerical simulations of calcium diffusion in a T-sensor[1] and experimentally from the chemical reaction between two compounds in two aqueous streams in a T-shaped microchannel, forming a fluorescent product.[12] Also in our 3D CFD simulations, this effect was clearly observed (Figure 8), and taken into account for the quantification of the glucose transfer.

Because the experiments were performed at residence times smaller than 1 s, the glucose concentrations in both the supply and receiving streams were still far from equilibrium when they were split again, ensuring high-mass-transfer rates. However, when in the experiments the interdiffusive zone is not split in the middle because of inequalities in the outflow rates, it causes differences between the measured and predicted glucose transfer. For example, when the outflow rate of the receiving stream is larger than the outflow rate of the feed stream, then a proportion of the glucose that is found in the receiving outflow port was not transferred via diffusion to this stream but ended up in the receiving stream because of the unequal outflow. Besides, unequal flow splitting should be prevented because it will, in the case of a recycle stream from/to a microbioreactor, result in draining or flooding of the reactor.

The effect of unequal outflow on the transfer of glucose to the receiving liquid was quantified with CFD simulations and the results are shown in Table 1. It can be inferred from this table that the amount of glucose in the receiving stream is very sensitive to nonequal flow splitting, especially at short residence times. This could be expected because at short residence times, the glucose profile perpendicular on the stream is very sharp at the liquid–liquid interface as can be seen in Figure 7. When, as a result of unequal outflow rates, this profile is not split straight in the middle, a
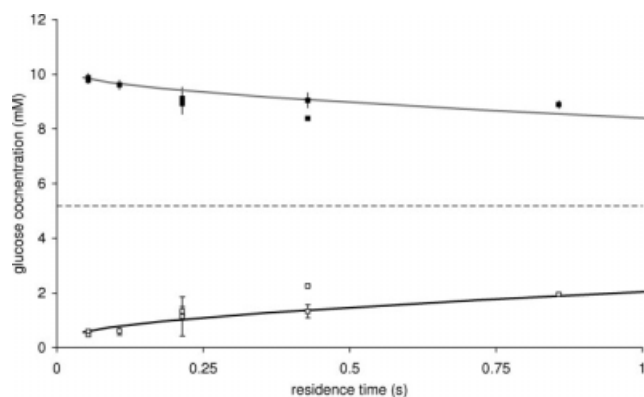
Figure 9. **Comparison of the measured glucose concentration at the exit ports of the feed and the receiving stream (■ and □, respectively) with the CFD simulations (gray line: feed stream; black line: receiving stream) at different residence times in the diffusion channel.**

The dashed line (---) indicates the equilibrium concentration. The error bars of the measurement points indicate the standard deviations of the measurements.

Figure 10. **Comparison of the experimental (based on feed (■) and receiving (□) streams) to CFD (—) results for glucose transport at different residence times.**

Glucose transport is expressed as total rate, as flux, or as volumetric feed rate to a 100 μL bioreactor.

relatively large amount of glucose is lost from or added to the receiving stream. At larger residence times, the glucose penetrates deeper into the receiving stream and the glucose concentration in the feed stream at the interface drops, thus reducing the effects of unequal flow splitting.

Equal flow splitting was checked experimentally by subsequently collecting and weighing the liquid from both outlet channels during a certain time interval. It must be noted that to ensure equal flow splitting serious attention should be paid to remove gas bubbles or particles that could restrict one of the flows as well as to the precise fabrication of the H-shaped channel.

Triplicate measurements resulted in a difference in volumetric outflow between both exits of 1.25% ± 0.6% (average ± standard deviation), which is much better compared with earlier findings of flow splitting.[6] This result significantly increases the practical applicability of these devices.

Quantification of the glucose transfer

Integration of the CFD simulations of the glucose concentration profiles after flow splitting yielded the predicted glucose concentrations in both outlet streams. The glucose concentrations in both streams were also determined experimentally for five different residence times, namely 54, 107, 214, 428, and 857 ms. Therefore, half a dozen samples were taken successively from both outlets over a time period of multiple hours for each residence time. It was found that after reaching a steady state, the concentrations at both outlets did not change significantly during multiple hours (data not shown). The simulated and experimentally determined glucose concentrations in both streams are plotted as a function of the residence time in Figure 9. It can be seen from this figure that the relation between the glucose concentrations in both streams and the residence time in the diffusion channel, obtained from the CFD calculations, compared very well with the experimental results. Furthermore, the obtained results confirm that partitioning of the glucose over both streams is still far from equilibrium.

The glucose transfer in the microdevice at different residence times was calculated from the concentration differences in the inlet and outlet streams. Complementary mass transfer rates were calculated based on the concentration data obtained from the feed and the receiving stream. The
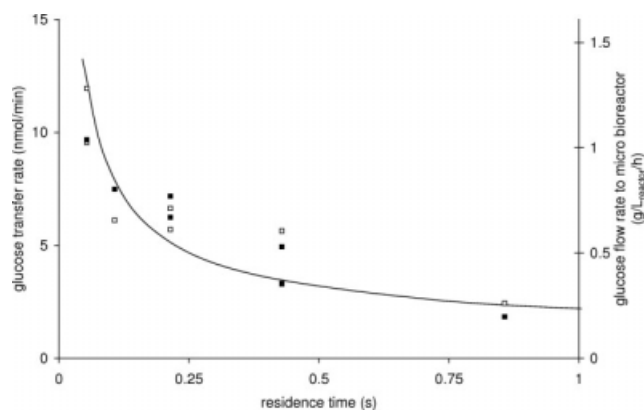
measured glucose transfer rates were found to be reproducible and corresponded well with the data obtained by the CFD simulations (Figure 10). From the good correspondence between the experimental data and the CFD results, it can be concluded that we have obtained a better understanding of the physical processes occurring in LFDI devices, compared with previous findings reported in literature.[6]

For a glucose concentration in the feed stream of 10.4 mM, mass transfer rates of 2.4–11.9 nmol/min were obtained for average residence times of 54–857 ms, respectively. It can be seen from Figure 10 that the average glucose transfer rate decreased at increasing residence times. The reason for this is that the glucose concentration gradient at the contact plane, and thus the driving force, decreases at increasing residence times, resulting in a decreasing mass transfer rate.

Because of the high-specific-area of the diffusion surface of the LFDI, i.e., 11.2×10^3 m^2/m^3, the glucose flux appeared to be high (0.73–3.58 mol m^2 h^{-1}) taking into account the relatively small concentration of glucose in the feed streams in our experiments.

If the LFDI would be applied for substrate feeding to a 100 μL microbioreactor, glucose feed rates ranging from 0.26 to 1.3 g $L_{reactor}^{-1}$ h^{-1}, could be achieved, which is sufficient to perform microbial fed-batch cultivations at relatively high-biomass-concentrations.

It can be concluded from the above results that CFD simulation is a powerful tool for estimating the mass transfer in an LFDI, even at very short residence times. For an even closer match between simulation and experiment, in the CFD simulations the flow velocity profile at the upstream position of the diffusion channel should be improved.

Conclusions

A laminar fluid diffusion interface (LFDI) device with a specific interfacial area for mass transfer of 11.2×10^3 m^2/m^3 was fabricated from glass. The mass transfer of glucose between cocurrent flowing water streams in the diffusion channel of the device was used as a model system to quantitatively investigate the mass transfer over the liquid–liquid interface. Residence times in the diffusion channel of less than 1 s were applied, ensuring high-mass-transfer rates. Proper flow splitting was achieved at the exit of the diffusion channel.

The measured glucose concentrations in both outlet ports at a fixed flow rate were found to be very stable in time and reproducible over multiple experiments. From the measured concentration differences, glucose transfer rates of 2.4–11.9 nmol/min, and glucose fluxes of 0.73–3.58 mol m^{-2} h^{-1} were calculated for average residence times of 54–857 ms and at a glucose concentration in the feed of 10.4 mM.

CFD simulations provided detailed information on the flow patterns as well as the glucose concentration profiles and resulting mass transfer rates in the diffusion channel of the device.

From the good agreement between the experimental and computational results for glucose transfer, it can be concluded that CFD simulations are a powerful and reliable tool for predicting the mass transfer in LFDI devices, even at relatively short residence times.

The obtained results contribute to an increased understanding of the mass transfer in LFDI devices, thus improving their applicability for the fast and controlled transfer of compounds between two liquid streams. An interesting application of LFDI devices could be the substrate feeding to microreactors. Measured glucose transfer rates for our LFDI device appeared sufficient to perform microbial fed-batch cultivations in a 100 μL bioreactor.

Acknowledgments

Literature Cited

1. Kamholz AE, Yager P. Theoretical analysis of molecular diffusion in pressure-driven laminar flow in microfluidic channels. *Biophys J*. 2001;80:155–160.

 2. Shui LL, Eijkel JCT, Van den Berg A. Multiphase flow in micro- and nanochannels. *Sens Actuators B Chem*. 2007;121: 263–276.

 3. Whitesides GM. The origins and the future of microfluidics. *Nature*. 2006;442:367–418.

 4. Maruyama T, Uchida JI, Ohkawa T, Futami T, Katayama K, Nishizawa KI, Sotowa KI, Kubota F, Kamiya N, Goto M. Enzymatic degradation of *p*-chlorophenol in a two-phase flow microchannel system. *Lab Chip*. 2003;3:308–312.

 5. Kenis PJA, Ismagilov RF, Whitesides G. Microfabrication inside capillaries using multiphase laminar flow patterning. *Science*. 1999;284:83–85.

 6. Hotta T, Nii S, Tajima T, Kawaizaumi F. Mass transfer characteristics of a microchannel device of split-flow type. *Chem Eng Technol*. 2007;30:208–213.

 7. Brody JP, Yager P. Diffusion-based extraction. *Sens Actuators B Chem*. 1997;58:13–18.

 8. Jandik P, Weigl BH, Kessler N, Cheng J, Morris CJ, Schulte T, Avdalovic N. Initial study of using a laminar fluid diffusion interface for sample preparation in high-performance liquid chromatography. *J Chromatogr A*. 2002;954:33–40.

 9. Oakey J, Allely J, Marr DWM. Laminar-flow-based separations at the microscale. *Biotechnol Prog*. 2002;18:1439–1442.

10. Weigl BH, Bardell RL, Kesler N, Morris CJ. Lab-on-a-chip sample preparation using laminar fluid diffusion interfaces-computational fluid dynamics model results and fluidic verification experiments. *Fresenius J Anal Chem*. 2001;371:97–105.

11. Lam YC, Chen X, Yang C. Depthwise averaging approach to cross-stream mixing in a pressure-driven microchannel flow. *Microfluid Nanofluidics*. 2005;1:218–226.

12. Ismagilov RF, Stroock AD, Kenis PJA, Whitesides G, Stone HA. Experimental and theoretical scaling laws for transverse diffusive broadening in two-phase laminar flows in microchannels. *Appl Phys Lett*. 2000;76:2376–2378.

13. Hermes DC, Heuser T, van der Wouden EJ, Gardeniers JGE, van den Berg A. Fabrication of microfluidic networks with integrated electrodes. *Microsyst Technol*. 2006;12:436–440.

14. Lee SC, Lee KH, Hyun GH, Lee WK. Continuous extraction of penicillin G by an emulsion liquid membrane in a countercurrent extraction column. *J Memb Sci*. 1997;124:43–51.

15. Venkatanarasaiah D, Varma YBG. Dispersed phase holdup and mass transfer in liquid pulsed column. *Bioprocess Eng*. 1998; 18:119–126.